



Comparison of PPP and RTK under static and dynamic scenarios

Authors:

Han Sun & Yue Pan

Supervisors:

Roland Hohensinn & Gregor Möller

May 2020

Abstract

RTK (real-time kinematics) and PPP (precise point positioning) are two main solutions to achieve high accuracy real-time positioning. In this project, we compare the performance of these two strategies under both static and dynamic scenarios. The comparing experiments are done by two popular software: RTKLIB and PPP WIZARD. Post-processing solution computed by PRIDE PPP-AR is used as ground truth. Considerable experiments indicate the following conclusions. Under static scenario, both RTK and real-time PPP can reach the accuracy of sub-cm level measurement noise and horizontal positioning bias. Besides, real-time PPP has slightly better performance than long baseline RTK. Under dynamic scenario, the measurement noise of RTK and PPP are on the same order of magnitude with their static counterpart, showing RTK and PPP's feasibility on dynamic application. By studying two time series during the earthquake, it is verified that both real-time PPP and RTK have the capacity to monitor the co-seismic displacement and their results agree within 2cm.

Content

1	Introduction	4
2	Methods	4
2.1	RTK	4
2.2	PPP	5
2.2.1	Introduction to PPP	5
2.2.2	Integer Clock Model	6
3	Data and Experiments	7
3.1	Data	7
3.2	Experiment Setup	8
3.2.1	RTKLIB for RTK	8
3.2.2	PPP WIZARD for real-time PPP	9
3.2.3	PRIDE PPP-AR for post-processing PPP	10
4	Results and Discussion	11
4.1	Experiment Results on Static Dataset	11
4.1.1	RTK with different baseline length	11
4.1.2	Real-time PPP	14
4.1.3	Comparison and analysis	15
4.2	Experiment Results on Dynamic Dataset	16
4.2.1	Comparison and analysis	16
4.2.2	Seismic monitoring by RTK and real-time PPP	17
5	Conclusion and Outlook	18
5.1	Conclusions	18
5.2	Future works	18
Annex	19	
List of References		19

1 Introduction

RTK and PPP are among the most precise positioning techniques with GNSS (global navigation satellite system). Due to different theories behind these two methods, they both have their own advantages and limitations.

RTK carrier phase differential technology is a differential method that processes the carrier phase observations of two measurement stations in real time, sends the carrier phase observation collected by the base station to the user receiver, and calculates coordinates by differenced measurements. Previously, only post-processing methods are available to solve both static and dynamic measurements to obtain centimetre-level accuracy. RTK is a new method that can obtain centimetre-level positioning accuracy on the field in real time. This benefits engineering setting out, topographic mapping, and various control measurements, which greatly improves work efficiency.

The main limitation of RTK is baseline length. For short and medium baseline, the error terms could be eliminated by applying simple strategies such as employing double-difference (DD) measurements and dual-frequency measurements. Also, network-RTK technique could be used to cancel the error terms. However, for long baseline over 100 km, RTK positioning faces difficulties which is not expected in conventional solutions. The error terms in double-difference equations caused by broadcast ephemeris errors, troposphere delay and earth tides effects are not negligible. Due to these remaining errors, the integer ambiguities are hard to be fixed. Meanwhile, the corresponding longer initialization time causes difficulty to determine precise real-time position, especially for hand-held moving devices.

PPP is another popular strategy for point positioning. It refers to users using the carrier phase and pseudocode range observations of a GNSS receiver, using high-precision satellite orbit and clock difference products, and carefully considering the influence of satellite, signal propagation path and receiver-related errors on positioning to achieve high-accuracy positioning. Compared to RTK, it does not require base station for baseline solution, which means users could get precise position based on a single receiver, without limitation of baseline length. Due to the above reason, PPP is more flexible and convenient, especially for hand-held moving devices. Before PPP, the only way to achieve high-accuracy positioning is difference positioning. PPP provides a new method for global high-accuracy GNSS positioning.

Due to the single-receiver strategy of PPP, FCBs (fractional cycle bias) absorbed into the undifferenced ambiguities could not be eliminated by double-difference strategy, thus destroying the integer property of ambiguities. Traditional PPP looks for float solutions of ambiguities only. This deficiency greatly decreases the accuracy of PPP and causes long initialization problem. If special strategies could be applied to recover the integer property of ambiguity, the positioning quality could be greatly improved.

To sum up, AR (ambiguity resolution) fixing is a key technique for both RTK and PPP to obtain rapid and precise solutions. For both methods, special integer ambiguity resolution strategies are required.

2 Methods

2.1 RTK

For long baseline RTK, the error terms in DD equation caused by broadcast ephemeris errors, troposphere delay and earth tides effects have significant impact on solution accuracy due to the long distance between base station and rover station. As the length of the baseline increases, the spatial correlation is greatly reduced, which in turn affects the fast resolution of integer ambiguity.

In this project, we experiment on a new strategy to deal with long RTK baseline over 100 km. First, original observations instead of linear combinations are used to suppress the noise. Second, the

ionosphere terms, which could not be eliminated by double-difference measurements due to the long baseline length are estimated by EKF (extended Kalman Filter), as well as other unknowns including troposphere error terms and float ambiguities. Then the estimated float ambiguities by EKF are resolved by existing efficient integer vector search strategy under ILS condition (LAMBDA and its extension MLAMBDA are used as integer search strategies).

By using EKF, a state vector and its variance-covariance matrix could be estimated with a measurement vector. The EKF formula could be solved combined with RTK-GPS equation to obtain the estimated state vector. In the strategy, the estimated states by EKF include the rover receiver ECEF position, single-differenced slant ionosphere delay for each satellite, tropospheric ZWD (zenith wet delay) and gradient parameters at the rover and base station sites and float ambiguities for dual-frequency carrier phases.

The estimated float ambiguities by EKF are resolved by integer vector search. During the EKF solution, single-difference is used instead of double-difference for carrier phase ambiguities to avoid the hand-over problem of reference satellites. Therefore, after obtaining the float estimated states by EKF, one more step needs to be implemented to transform the single-differenced ambiguities into double-differenced form before starting integer vector searching process. This searching process employs the LAMBDA and MLAMBDA strategy.

In addition, to improve the fixing ratio, “partial fixing” and “fix and hold” modes are employed. By applying ‘partial fixing’, only float ambiguities of satellites above a threshold of elevation are fixed to integer terms. ‘fix and hold’ refers to tight constraint to fixed ambiguities.

2.2 PPP

2.2.1 Introduction to PPP

Integer ambiguity resolution fixing is crucial in improving PPP accuracy. As PPP is solved for a single receiver, no double-difference measurements are available. The fractional-cycle biases in the GPS measurements which are absorbed by the undifferenced ambiguity estimations destroy the integer property. Traditionally, ambiguities in PPP are fixed to float values due to this problem. However, if the ambiguities could be fixed to integers, the accuracy would be improved greatly. There are a variety of methods managing to remove the phase bias and recover the integer property of PPP ambiguity resolution. They could be divided into two main categories: ‘integer-recovery clocks’ (IRC)-base methods and FCB-based methods.

IRC-based methods aim to drive the estimated phase bias into integer clock estimates. These methods estimate the integer-recovery clocks by fixing the undifferenced ambiguities to integers in advance. Integer clock model belonging to this kind of strategy is employed in PPP WIZARD. In this model, the undifferenced ambiguity measurements are decomposed into wide-lane part and narrow-lane part, and directly fixed to integers. An arbitrary value is assigned to the FCB of receiver to get the FCB of the satellite. Then the wide-lane phase bias, which is considered stable over a few days or even a few months, is estimated by averaging the fractional part derived from Melbourne-Wubbena (MW) combination. The remaining narrow-lane part is then fixed to integers and assimilated into clock estimates. The narrow-lane phase bias is considered instable and mean value within a short period (less than 15 min) needs to be computed to achieve high-accuracy solutions.

FCB-based methods estimate the FCBs by averaging the fractional part of the float ambiguity estimates. In PRIDE PPP-AR, UPD (uncalibrated phase delay) model belonging to this category is employed. In this strategy, the undifferenced ambiguity measurements are decomposed and the difference value between satellites are used to eliminate the FCBs of receivers instead of directly fixing the ambiguity values to integer values. The wide-lane part is fixed the same way as integer clock model. But for the narrow-lane FCB fixing, the same method of fixing wide-lane part is applied again.

Besides strategies to fix integer ambiguities, another focus point of PPP is how to obtain real-time solutions. In the aspect of positioning model and methods, there is no essential difference between real-time PPP and post-processing PPP. The main difference lies in practical implementation. To obtain real-time

solution, real-time high-accuracy satellite orbit products and clock difference products should be available, and users should have access to these products via internet or satellite communication link.

2.2.2 Integer Clock Model

This method manages to recover the integer property of ambiguity of PPP by clock difference estimation. First, it estimates the wide-lane phase bias of undifferenced measurements. Then the narrow-lane part is absorbed into the satellite clock difference. By introducing IRC satellite clock difference corrections, the integer property of ambiguities is recovered, and then the ambiguities could be fixed using traditional methods. CNES provides publicly products of wide-lane UPD and integer clock products.

To get the integer ambiguity resolution, there are two main steps. First, network solution needs to be implemented to compute the integer clock product which is required from the user end. Then the clock product will be provided to users for their own PPP solution.

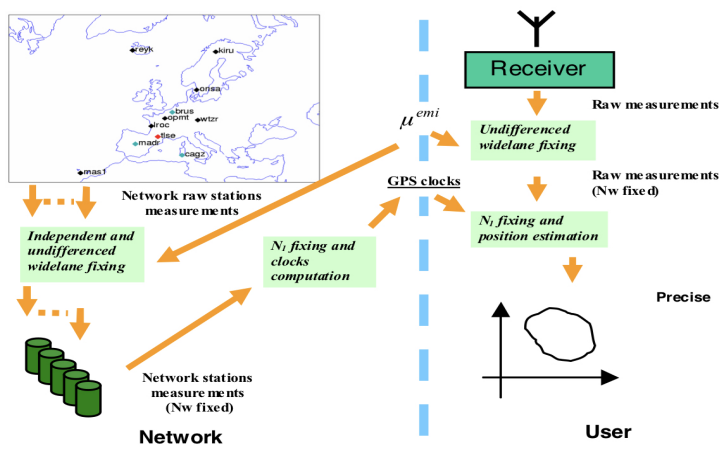


Figure 1. Integer clock model solution procedure

During the network solution, first the wide-lane ambiguity derived from MW combination is fixed independently for each receiver of the network using previously determined satellite delays. This could lead to the ionosphere-free equations where the only ambiguity left is the ambiguity on the first frequency. Then the remaining ambiguities are fixed globally over the whole. As a result, the by-product called the integer phase clock could be obtained for the GPS constellation. The narrow-lane phase bias is driven into the clock estimations and the product could then be broadcasted to the users.

On the user side, the same first processing step is applied to any receiver to fix its zero differenced integer wide-lane ambiguities using the same satellite delays as the ones used in the network solution. And then the integer phase clocks are employed to fix the remaining ambiguities on the first frequency relating to absolute centimetre level PPP.

For the extension of real-time positioning, specific strategies should be applied to adapt to the real-time context. Wide-lane ambiguities at the receiver level can usually be fixed after 5 to 30 minutes, which depends on the appropriate averaging window length and the quality of the pseudo-range measurements. Although fast solution is expected in real-time application, an averaging time window with certain length is required to reduce the effect of measurement noise. The noise level is closely connected with the quality of pseudo-range measurements, which is directly correlated with elevation angles. In cases for high-quality solutions, a threshold of 30 degrees of elevation angle could be set in this method.

To fix the narrow-lane phase bias, an EKF is implemented to compute the integer phase clock over the whole network. The state of vector is estimated including all the satellite and station clocks, zenith troposphere delay and float ambiguities. After the wide-lane phase bias are fixed to their integer values, narrow-lane phase bias could be obtained in the filter. They are fixed to the closest integer value of the float solution or an arbitrary integer value, depending on the available measurements. The satellite clock with the closest covariance to the measurement noise is selected as integer phase clock by-product for each time step.

3 Data and Experiments

3.1 Data

The dataset used in this project is the high-rate GPS data archive of the 2016 central Italy seismic sequence provided by Istituto Nazionale di Geodisca e Vulcanologia. The central Apennines (Italy) have been struck by a huge and long seismic sequence including 5 moderate magnitude earthquakes (5.4-6.5) and about 45000 aftershocks.

Date	Original Time (UTC)	Latitude(DD.dddd)	Longitude(DD.dddd)	Depth(km)	Mw
2016-08-24	01:26:32.00	42.6983	13.2335	8.1	6.0
2016-08-24	02:33:28.00	42.7922	13.1507	8.0	5.4a
2016-10-26	17:10:36.34	42.8802	13.1275	8.7	5.4b
2016-10-26	19:18:05.85	42.9087	13.1288	7.5	5.9
2016-10-30	06:40:17.36	42.8322	13.1107	9.2	6.5

Table 1. Information of 5 main shocks of 2016 central Italy seismic sequence

The strongest earthquakes have been recorded by high-rate sampling (from 1s to 0.05s) continuous Global Positioning System (HRGPS) stations belonging to several networks developed for both scientific and surveying purposes. In this project, we are going to analyse measurements under both static and dynamic scenarios. For static data analysis, measurements on November 1, 2016, day after the final earthquake, are used. The period is from 9:00 to 13:00 PM. The observation station MSAN is chosen as the rover station as it is closest to the earthquake centre. For RTK solution, 3 stations with various distance from the rover station are chosen as base stations. For dynamic data analysis, we choose the earthquake that took place on the 26th of October 2016 at 17:10. The period is from 16:00 to 19:30, during which another moderate earthquake of 5.9 also happened. We choose the same period on the 24th of October 2016 for static comparison.

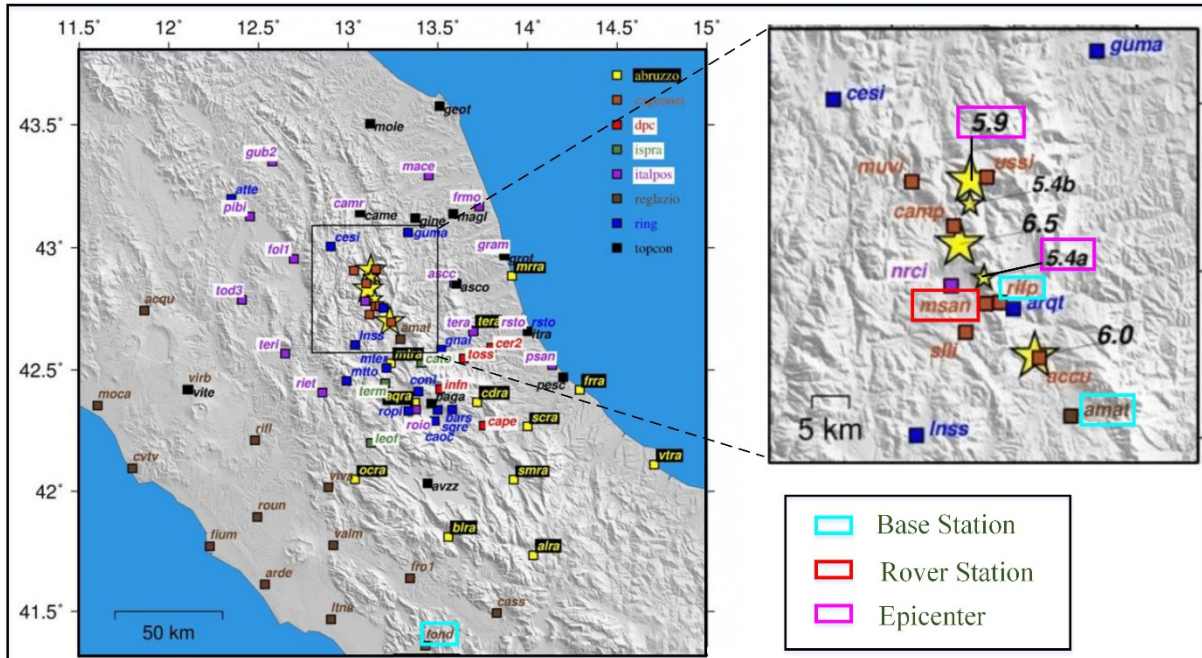


Figure 3. Central Italy Earthquake Dataset, Figure from: [<http://ring.gm.ingv.it/>]

Frequency		1Hz
Duration		1/11/2016(DOY306) 09:00-13:00
Rover Station		MSAN
Base Station	RIFP	≈ 1km to MSAN, short baseline
	AMAT	≈ 20km to MSAN, medium baseline
	FOND	≈ 170km to MSAN, long baseline

Table 2. Information of static dataset

Frequency	10Hz
Duration	Dynamic: 26/10/2016 (DOY300) 16:00-19:30
	Static Reference: 24/10/2016 (DOY298) 16:00-19:30
Rover Station	closest to the epicenter (≈ 10km): MSAN
Base Station	farthest from the epicenter (≈ 175km): FOND

Table 3. Information of dynamic dataset: 5.4b earthquake of October 26, 2016

3.2 Experiment Setup

3.2.1 RTKLIB for RTK

RTKLIB is an open source program package for standard and precise positioning with GNSS and it supports all kinds of positioning modes for both real-time and post-processing such as SPP, DGNSS, RTK, PPP-Kinematic, PPP-Static and PPP-Fixed [2]. Since there are considerable options to play with for RTK with various baselines and the related documents are available, RTKLIB is selected as the software for conducting RTK in this study. We adopted different RTK strategy for different baseline lengths according to [1], as shown in Table 4. Generally, the longer the baseline is, the more caution should be taken on the parameter settings.

Baseline length		Error elimination strategy			
		Ephemeris	Ionosphere	Troposphere	Others
Short	<10km	Broadcast	-	Saastamoinen	-
Medium	10-100km	Broadcast	Dual frequency	Saastamoinen	-
Long	>100km	Real-time precise (IGU)	Dual frequency	Estimate ZTD+MF	Earth tides

Table 4. Different RTK baselines and corresponding strategies

For long baseline RTK, regarding to the satellite ephemeris, the IGS ultra-rapid (IGU) precise satellite ephemeris are downloaded and the predicted parts are extracted so that the real-time property can be achieved [3]. We use the same configuration as described in [1]. The options and products we used for long baseline RTK are shown in Table 5.

Option	Setting
Positioning Mode	Kinematic
Frequencies	L1+L2+L5
Satellite	GPS, GLONASS, Galileo
Receiver Dynamics	Off (Static Dataset), On (Dynamic Dataset)
Base Station Coordinate	Solution of Pride PPPAR
Earth Tides Correction	Solid & Ocean Tide Loading
Elevation Mask	7°
Ionosphere Correction	Estimate STEC
Troposphere Correction	Estimate ZTD + Gradient
Satellite Ephemeris	Real-time Precise (IGS Ultra-rapid)
Ambiguity Validation Threshold	3.0
Integer Ambiguity Resolution Strategy	Fix and Hold
Min Elevation to Fix Ambiguity	25°
Min Elevation to Hold Ambiguity	35°
Code/Carrier-Phase Error Ratio	100
Carrier Phase Error	$0.003 + 0.003 / \sin El$ m
Process Noise of Vertical Iono. Delay	10^{-3} m/sqrt(s)\$
Process Noise of ZTD	10^{-4} m/sqrt(s)\$
Satellite Antenna Model	IGS14.ATX
Receiver Antenna Model	IGS14.ATX
EOP File	IGU Earth Orientation Parameters

Table 5. Parameter settings of RTPOST in RTKLIB for long baseline RTK

3.2.2 PPP WIZARD for real-time PPP

PPP WIZARD is a partial open-sourced toolbox used for real-time PPP operations. Based on the accurate orbits, clocks and phase bias products for GPS and GLONASS published by CNES GNSS analysis centre, it is reported that PPP WIZARD adopts the ‘undifferenced ambiguity resolution’ technology to achieve real-time PPP with the horizontal accuracy of 1cm. We use the configurations as shown in Table 6 according to [4].

Option	Setting
Positioning Mode	PPP AR
Satellite	GPS, GLONASS, Galileo
Model position noise (m)	10 (Dynamic Dataset), 0.02 (Static Dataset)
Satellite Ephemeris	CNES precise ephemeris *sp3
Satellite Clock	CNES precise clock *clk
Satellite Bias	CNES Code and Phase Biases for satellites *bia
Differential Code Bias	P1C1,P1P2,P2C2.dcb
Tropo. initial noise(m)	0.5
Iono. rejection threshold(m)	5
Code rejection threshold(m)	10
Phase rejection threshold(m)	0.05
Satellite Antenna Model	IGS14.ATX

Table 6. Parameter settings of PPP WIZARD for real-time PPP

3.2.3 PRIDE PPP-AR for post-processing PPP

PRIDE PPP-AR is an open-sourced software aiming at accurate post-processing of GPS data. This software is mainly composed of the undifferenced processing module for float ambiguity estimation and the integer ambiguity resolution module. It is reported that PRIDE PPP-AR is able to achieve millimetre level RMS error for static applications and the ambiguity fixing ratio is more than 99%. We use the configurations as shown in Table 7 according to [5].

Option	Setting
Ambiguity fixing mode	FIX
Available positioning mode	Static
Remove bias	YES
Common observation time (s)	600
Cutoff angles for eligible ambiguities in AR (deg)	15
Differential Code Bias	P1C1, P2C2.dcb
Satellite ephemeris	CODE GNSS orbit *EPH
Satellite clock	CODE GNSS clock *EPH
Satellite Antenna File	igs14.atx

Table 7. Parameter settings of PRIDE PPP-AR for post-processing PPP

To verify and evaluate the performance of PRIDE PPP-AR, we conducted some experiments. We select four IGS sites that are most close to the studied area in Italy and download their observation files on the same day of the static dataset. Then we take the estimated coordinate of CODE'S final 3-day solution as the ground truth of the IGS stations and compare them with the solution of PRIDE PPP-AR using the mentioned configurations. The difference between PRIDE PPP-AR and CODE's estimations are shown in Table 8. Since the difference is within 2mm, PRIDE PPP-AR's solution is accurate enough as the ground truth position of the stations used in our experiment. The one-day solution of PRIDE PPP-AR on the four experimental sites (MSAN, RIFP, AMAT and FOND) are listed in Table 9. The output standard deviation is on the sub-mm magnitude, indicating the reliability of the solution.

Station	Location	δx (mm)	δy (mm)	δz (mm)
MATE	Matera, IT	1.1	0.7	0.4
M0SE	Roma, IT	0.8	0.6	0.9
NOT1	Noto, IT	1.3	0.5	0.7
PADO	Padova, IT	1.6	0.6	1.1

Table 8. Positioning accuracy of PRIDE PPP-AR on four IGS stations in Italy during the same period of the static dataset

Station	X(m)	Y(m)	Z(m)	std.X(mm)	std.Y(mm)	std.Z(mm)	Notes
MSAN	4567666.272	1067487.265	4308726.184	1.8	0.9	1.0	ROVER
RIFP	4567491.529	1069312.105	4309206.113	5.1	2.6	3.1	BASE(1km)
AMAT	4574948.639	1080829.780	4297745.196	1.4	0.9	0.8	BASE(20km)
FOND	4663468.185	1113756.262	4192232.917	1.0	0.7	0.6	BASE(170km)

Table 9. One-day solution of PRIDE PPP-AR on the four experimental sites

4 Results and Discussion

4.1 Experiment Results on Static Dataset

According to the strategy and parameter settings described in previous sections, we implemented RTK, real-time PPP on the static dataset.

4.1.1 RTK with different baseline length

The performance of RTK with different baseline length is tested on a 4-hour static time sequence. Three base stations are 1km (RIFP), 20km (AMAT) and 170km (FOND) away from the rover station (MSAN) respectively. The sampling ratio of the static dataset is 1Hz. The output of RTKLIB is in an Earth-Centred Earth-Fixed (ECEF) coordinate system. To have an intuitive cognition of the positioning error and better comparison between different solutions, we firstly convert the XYZ coordinate in ECEF to the East, North, Up (ENU) coordinate system of a reference point, as shown in Fig. 3. In RTKLIB, the reference point is the average positioning result over the time-series. Such E/N/U error can be used to analyse the convergence time and measurement noise but cannot be used to compare with other solutions and the ground truth.

Fig. 4 to Fig. 6 show the E/N/U errors relative to the average positioning coordinate as well as the integer ambiguity fixing ratio of short, medium, and long baseline RTK.

It is shown that, by applying double-differencing on two adjacent stations, it's relatively easy to resolve the integer ambiguity and the fixing ratio is about 98%. However, when the two stations are far away from each other, the condition on the signal propagation path would not be identical. Therefore, even by using additional products and various ambiguity fixing tricks, the integer ambiguity fixing ratio is relatively low in a short period for long baseline RTK.

However, as shown in Fig.7, by extending the time series to a longer period, the fixing ratio of long baseline RTK improves from 34% to 82%, thanks to the “fix and hold” ambiguity resolution strategy. The strategy indicates that a fixed ambiguity would be held to an integer value until a cycle-slip occurs [1].

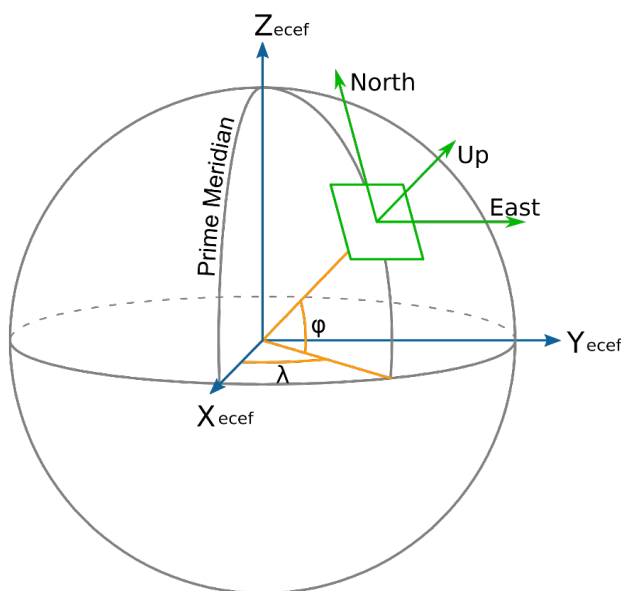


Figure 3. ECEF XYZ and station NEU coordinate systems

Regarding to the measurement noise of RTK, Table 10 indicates that even the long baseline RTK's measurement noise is under 5 cm. Besides, the noise is much larger on the vertical direction for various baseline lengths.

Baseline length (km)	fixing ratio	average std.(cm)		
		E-W	N-S	U-D
1 (short)	98%	0.5	0.2	1.2
20 (medium)	72%	1.0	0.3	2.6
170 (long)	34%	0.9	0.4	4.2

Table 10. Ambiguity fixing ratio and standard deviation of RTK with different baseline lengths on the static dataset

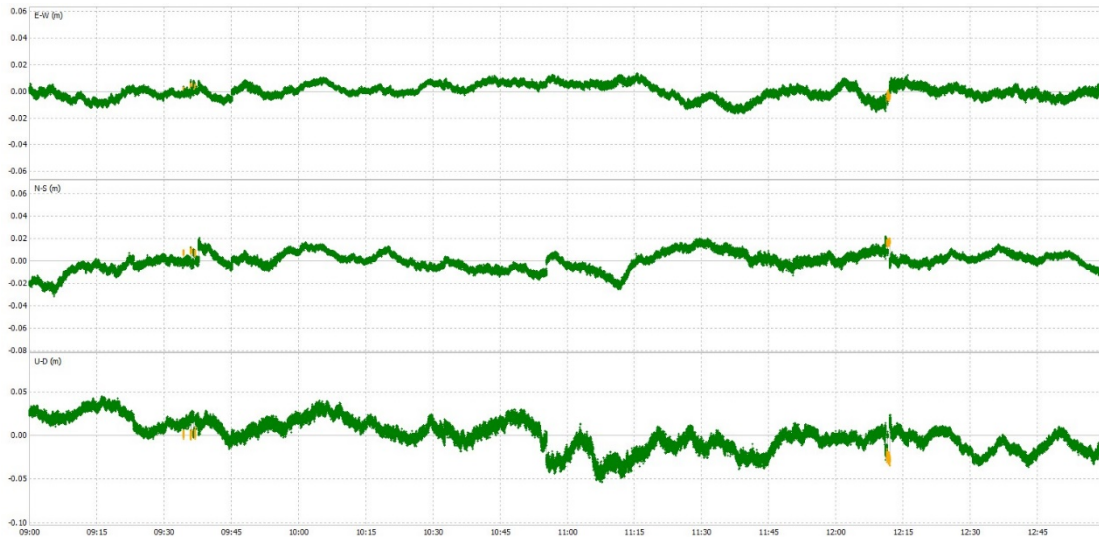


Figure 4. E/N/U errors (taking the mean positioning coordinate as reference) of short baseline RTK (rover: MSAN, base: RIPP, baseline length: 1km) over 4 hours (green: integer ambiguity fixed, yellow: integer ambiguity not fixed)

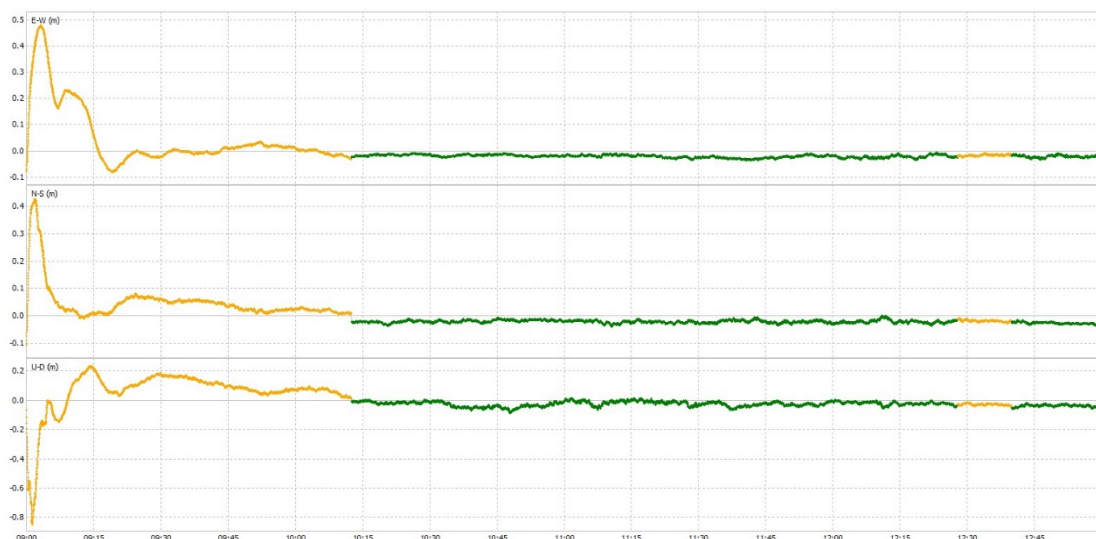


Figure 5. E/N/U errors (taking the mean positioning coordinate as reference) of medium baseline RTK (rover: MSAN, base: AMAT, baseline length: 20km) over 4 hours (green: integer ambiguity fixed, yellow: integer ambiguity not fixed)

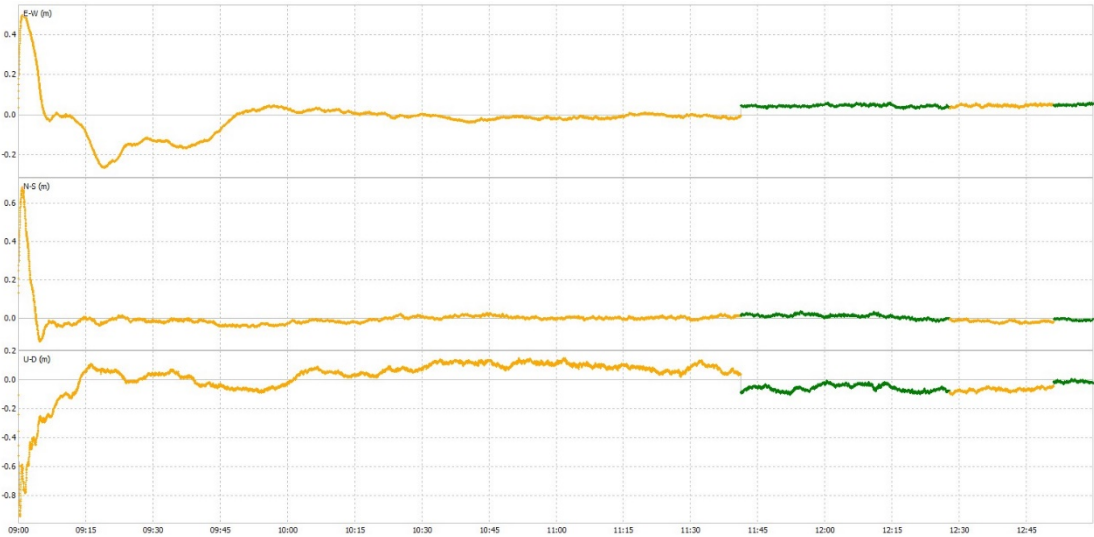


Figure 6. E/N/U errors (taking the mean positioning coordinate as reference) of long baseline RTK (rover: MSAN, base: FOND, baseline length: 170km) over 4 hours (green: integer ambiguity fixed, yellow: integer ambiguity not fixed)

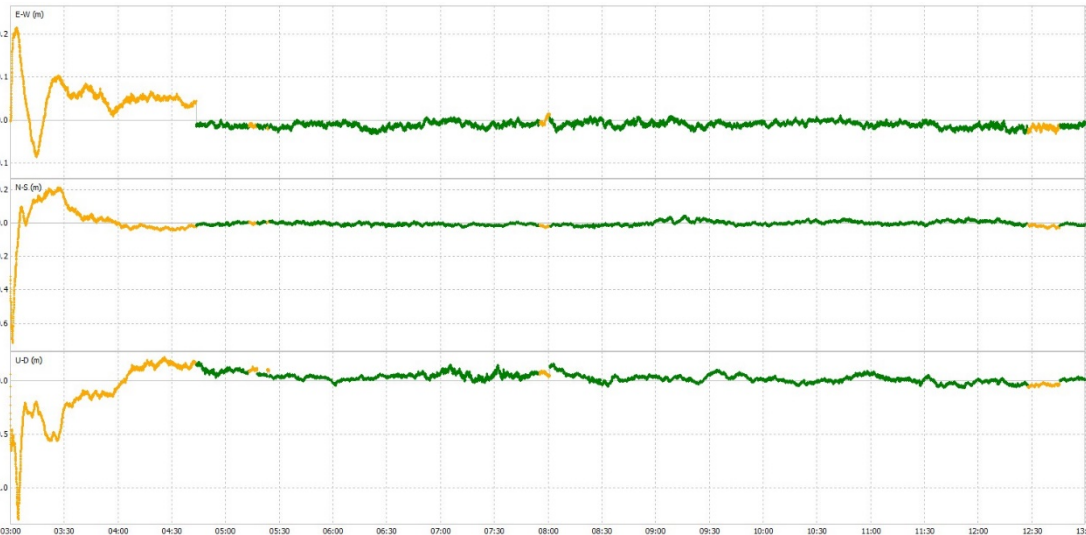


Figure 7. E/N/U errors (taking the mean positioning coordinate as reference) of long baseline RTK (rover: MSAN, base: FOND, baseline length: 170km) over 10 hours (green: integer ambiguity fixed, yellow: integer ambiguity not fixed)

To compare the performance of different real-time positioning solutions under a common frame, the positioning result of post-processing PPP on the same day is set as the reference point of NEU coordinate system.

Long baseline RTK	E(cm)	N(cm)	U(cm)
final bias	1.9	1.2	33.7
final std.	0.6	0.2	1.8

Table 11. Bias and standard deviation of the last epoch for long baseline RTK under static scenario

For the long baseline RTK, As shown in Table 11, the standard deviation of the last epoch on E, N and U direction are all smaller than 2 cm. The E and N bias are smaller than 2 cm while the vertical bias is 33.7 cm. From Figure 8, it is shown that that the bias on Up direction remains through the whole time series.

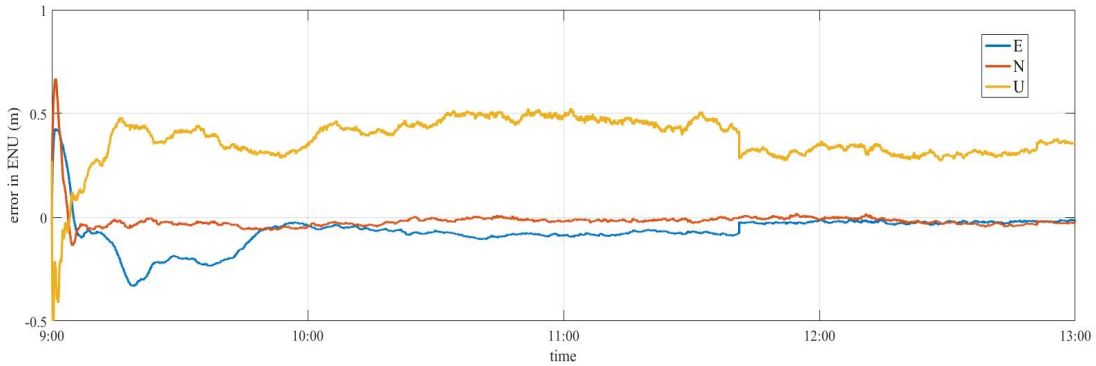


Figure 8. Long baseline RTK's E/N/U positioning error under the static scenario (taking post-processing PPP's result as ENU reference point)

4.1.2 Real-time PPP

In this section, we show the positioning results of real-time PPP under static scenarios.

As shown in Fig. 9, though the number of available satellites is low, for most of the observations the wide-lane ambiguity is fixed while for half of the observations, the narrow-lane ambiguity is fixed, which seems to agree with PPP WIZARD's principle. However, it is shown in Fig. 10 that the positioning result on vertical direction is not good. There's obvious vertical jump near the end of the time series, which indicates a cycle slip during those epochs. Though there is a decimetre level vertical bias, the standard deviation on E/N/U are all within 3 cm and the horizontal bias is within 5cm, as shown in Table 12.

Real-time PPP	E(cm)	N(cm)	U(cm)
final bias	0.4	4.3	55.1
final std.	0.7	0.1	3.3

Table 12. Bias and standard deviation of the last epoch for Real-time PPP under static scenario

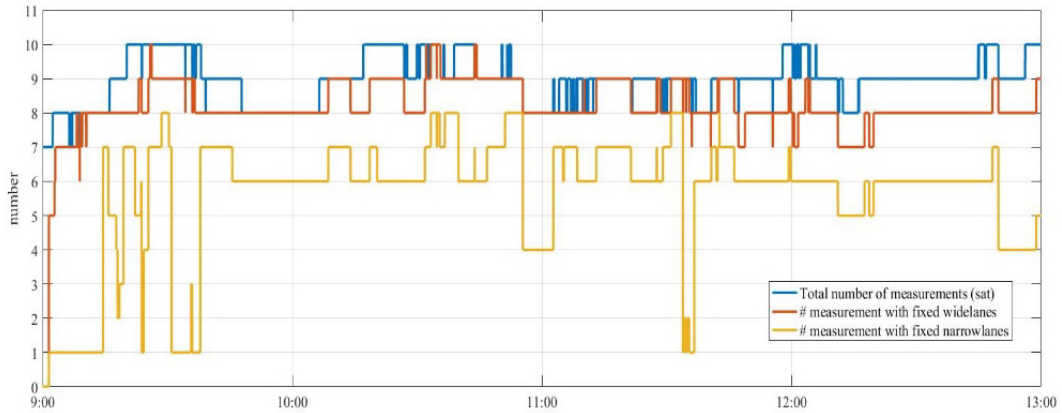


Figure 9. Number of measurements with fixed wide lane and narrow lane ambiguity during the 4-hour static time series.

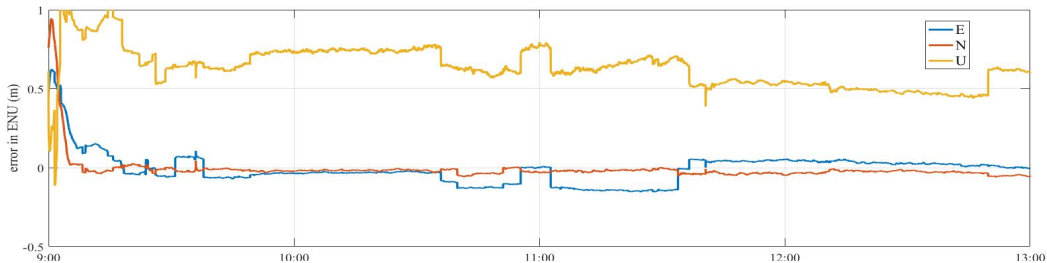


Figure 10. Realtime PPP's E/N/U positioning error under the static scenario (taking post-processing PPP's result as ENU reference origin)

4.1.3 Comparison and analysis

In this section, we compare RTK with different baseline lengths and real-time PPP under the same E/N/U reference system. To verify the real-time PPP solution, we adopt the real-time PPP function implemented in RTKLIB using the same products published by CNES. It is found that RTKLIB and PPP WIZARD's PPP results agree within 1 cm after convergence. Table 13 indicates that Real-time PPP's measurement noise is larger than medium baseline RTK but smaller than long baseline RTK, which indicates that real-time PPP can act as a good alternative when the nearest base station is more than 100 km away from the rover.

As shown in the left part of Fig. 11, the convergence time is less than one hour for all the solutions. Fig. 12 and the right part of Fig. 11 show how the positioning results of different real-time solutions change during the time series.

Solution	average std. (cm)		
	E-W	N-S	U-D
RTK 1km (short)	0.5	0.2	1.2
RTK 20km (medium)	1.0	0.3	2.6
RTK 170km (long)	0.9	0.4	4.2
Real-time PPP	1.1	0.3	3.3

Table 13. the average standard deviation of RTK with various baseline lengths and real-time PPP during a 4-hour static time series

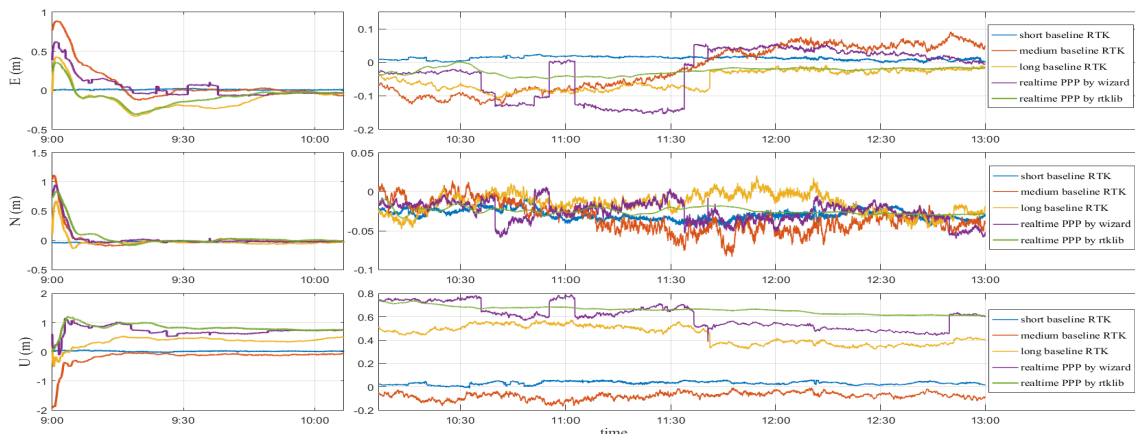


Figure 11. Comparison of RTK and real-time PPP on a static time series

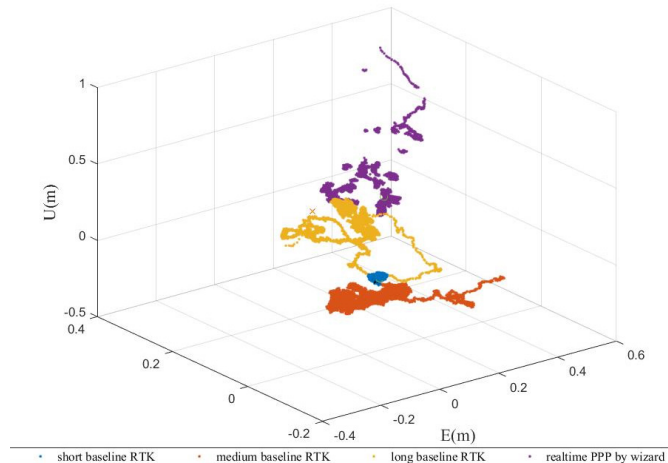


Figure 12. 3D Positioning trajectory of RTK and real-time PPP on the static dataset

4.2 Experiment Results on Dynamic Dataset

As described in section 3.1, the dynamic dataset covers two moderate earthquakes (Mw5.4b and Mw5.9) on October 26 in 2016 taking place in Central Italy. The rover station MSAN is about 10km away from the earthquake Mw5.4b's centre while the base station FOND is about 175km away from the earthquake Mw5.4b's centre. The sampling rate of the dataset is 10Hz. Since the baseline length is about 170km in this case, the long baseline RTK strategy is used.

4.2.1 Comparison and analysis

Firstly, we studied the measurement noise of RTK and real-time PPP under the dynamic scenario, as shown in Fig. 13. During the whole period, it is shown that the standard deviation of real-time PPP is slightly smaller than the long baseline RTK, which is consistent with the static case.

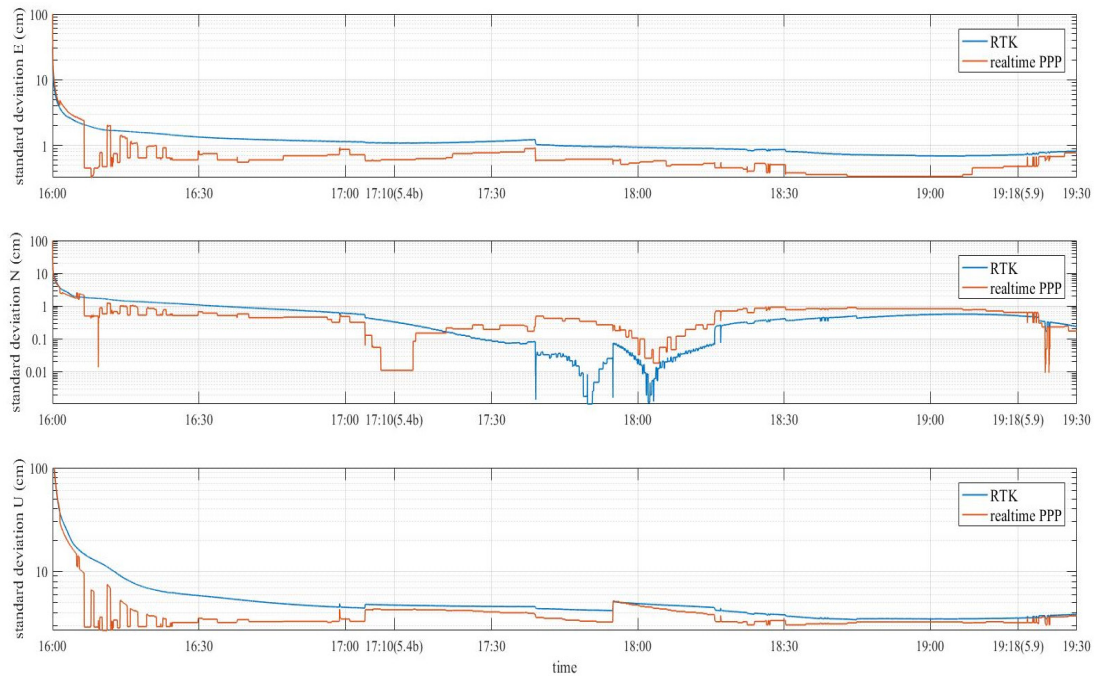


Figure 13. Comparison of real-time PPP and RTK's E/N/U standard deviation during a partial dynamic time series

The earthquake Mw5.4b took place at 17:10 on October 26, 2016, therefore we select a one-minute time series after the timestamp of the earthquake as the dynamic period. To have a fair comparison of PPP and RTK's performance under static and dynamic scenario, we select another one-minute time series exactly two days before the earthquake. There is no recorded earthquake on that day. The results are shown in Table 14, which indicate there is no significant increase of measurement noise during the earthquake for both real-time PPP and RTK.

	Solution	E(cm)	N(cm)	U(cm)
static std.	PPP	0.4	0.1	3.8
dynamic std.		0.6	0.1	4.2
static std.	RTK	1.1	0.5	4.3
dynamic std.		1.1	0.4	4.7

Table 14. Comparison of real-time PPP and RTK's measurement noise under static and dynamic scenarios

4.2.2 Seismic monitoring by RTK and real-time PPP

High-rate GNSS data has been proved to be useful for retrieving the co-seismic displacement and furnishing reliable waveform patterns for various seismological applications [6]. In this section, the one-minute time series round the time stamp of the main shock of two moderate earthquakes (Mw 5.4b and Mw 5.9 on October 26, 2016 in Central Italy) are studied, as shown in Fig. 14 and Fig. 15.

It is found that RTK and PPP agree within a value of 5 mm horizontally and 2cm vertically during the earthquake period. Besides, both RTK and PPP's solution indicates that the dramatic co-seismic displacement appears about 20 seconds after the main shock, which is consistently associated with the seismic waves' propagation.

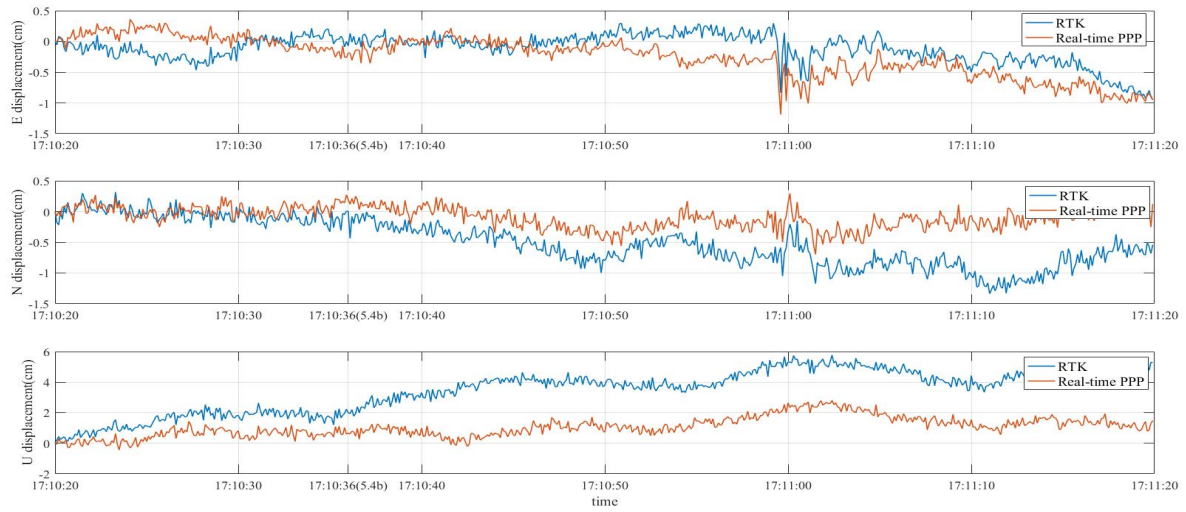


Figure 14. Comparison of RTK and real-time PPP on a one-minute time series of "Mw 5.4b" Earthquake on October 26, 2016

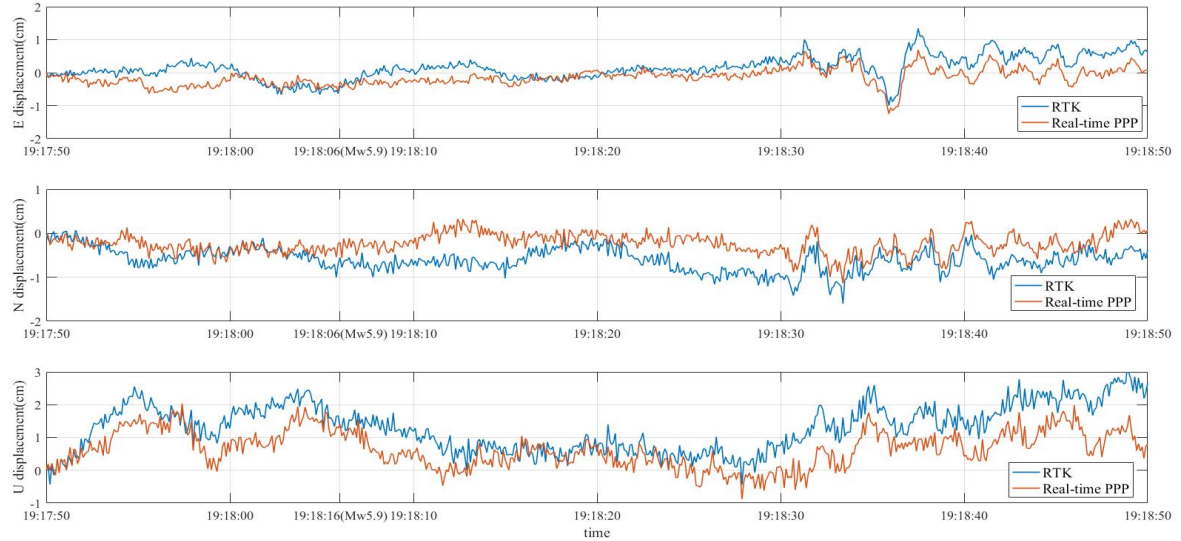


Figure 15. Comparison of RTK and real-time PPP on a one-minute time series of "Mw 5.9" Earthquake on October 26, 2016

5 Conclusion and Outlook

5.1 Conclusions

In this study, we compare the performance of two real-time GNSS positioning solutions, namely, RTK with different baseline lengths and real-time PPP.

Throughout the considerable experiments, the following conclusions can be drawn.

Firstly, as for the measurement noise, the standard deviation of all the compared solutions are within 5 cm. Specifically, real-time PPP is worse than short and medium baseline RTK but slightly better than long baseline RTK. Besides, the noise of all the compared solutions mainly lies on the vertical direction. Secondly, regarding to the horizontal measurement bias, almost all the compared solutions are less than 2 cm. The vertical bias of short and medium baseline RTK are less than 4cm while the value for long baseline RTK and real-time PPP are as large as a few decimetres. The results indicate that RTK and real-time PPP can handle the 2-dimensional measurement tasks but it might cause some problems for applications such as accurate levelling measurement.

Thirdly, the magnitude of noise on dynamic scenario is just a bit larger than it on static scenario, thus indicating the stable positioning ability of RTK and real-time PPP on dynamic applications such as vehicle localization and deformation monitoring.

Fourthly, we verified that both real-time PPP and RTK can be used to monitor the co-seismic displacement and their positioning results during the earthquake are consistent within 2cm.

5.2 Future works

From the experiments, we find the issue of decimetre magnitude vertical bias of long baseline RTK and real-time PPP, which differs from the reported performance of the software and related papers. Since we have verified the mm magnitude positioning accuracy of post-processing PPP (PRIDE PPP-AR) on several IGS stations in Italy during the same period as the static dataset, the ground truth adopted by us should be accurate. We suspected that the cause of the vertical bias of real-time PPP solved by PPP WIZARD might be the improper implementation of solid earth tide correction according to [4]. For long baseline RTK, the model and the estimation of troposphere and ionosphere parameters in RTKLIB may not be accurate enough due to the solar activity and the large variation of water vapor content [1]. Further effort would be made on the analysis of the variance-covariance matrix of the normal equation in least square parameter estimation, from which we might figure out the actual cause of the vertical bias.

What's more, since the software used in this project are all open-sourced (RTKLIB, PRIDE PPP-AR) or partial open-sourced (PPP WIZARD), the future work would be the secondary development based on the original functions to achieve the faster convergence and more reliable performance for long baseline RTK and real-time PPP.

Annex

List of References

1. Takasu T, Yasuda A. Kalman-filter-based integer ambiguity resolution strategy for long-baseline RTK with ionosphere and troposphere estimation, /Proceedings of the ION GNSS. 2010: 161-171.
2. Takasu, T. (2011). RTKLIB: An open source program package for GNSS positioning. Tech. Rep., 2013. Software and documentation.
3. Kouba, J. (2009). A guide to using International GNSS Service (IGS) products.
4. D. Laurichesse, F. Mercier, J.P. Berthias, P. Broca, L. Cerri, "Integer Ambiguity Resolution on Undifferenced GPS Phase Measurements and its Application to PPP and Satellite Precise Orbit Determination", Navigation, Journal of the institute of Navigation, Vol. 56, N° 2, Summer 2009
5. Geng, J. & Xingyu, Chen & Pan, Yuanxin & Mao, Shuyin & Li, Chenghong & Zhou, Jinning & Zhang, Kunlun. (2019). PRIDE PPP-AR: an open-source software for GPS PPP ambiguity resolution. GPS Solutions. 23. 10.1007/s10291-019-0888-1.
6. Avallone, A., Latorre, D., Serpelloni, E., Cavaliere, A., Herrero, A., Cecere, G., ... & Mattoni, M. (2016). Coseismic displacement waveforms for the 2016 August 24 Mw 6.0 Amatrice earthquake (central Italy) carried out from High-Rate GPS data. Annals of Geophysics, 59.
7. <http://ring.gm.ingv.it/>
8. Geng, J. & Xingyu, Chen & Pan, Yuanxin & Zhao, Qile. (2019). A modified phase clock/bias model to improve PPP ambiguity resolution at Wuhan University. Journal of Geodesy. 1-15. 10.1007/s00190-019-01301-6.
9. [D. Laurichesse., et al., 2008]: D. Laurichesse, F. Mercier, J.P. Berthias, J. Bijac, "Real Time Zero-difference Ambiguities Blocking and Absolute RTK", Proceedings of the ION NTM 2008, January 28-30, 2008, San Diego, California
10. Geng, J. & Meng, Xiaolin & Dodson, Alan & Teferle, Norman. (2010). Integer ambiguity resolution in precise point positioning: Method comparison. Journal of Geodesy. 84. 569-581. 10.1007/s00190-010-0399-x.
11. D.Laurichesse, A. Privat, "An Open-source PPP Client Implementation for the CNES PPP-WIZ-ARD Demonstrator", Proceedings of the ION GNSS+ 2015, September 2015, Tampa, Florida
12. P. Collins, S. Bisnath, F. Lahaye, P. Heroux, "Undifferenced GPS Ambiguity Resolution Using the Decoupled Clock Model and Ambiguity Datum Fixing", Navigation, Journal of the institute of Navigation, Vol. 57, N° 2, 2010